Synthesis and Characterization of a Novel Spin-Labeled Affinity Probe of Human Erythrocyte Band 3: Characteristics of the Stilbenedisulfonate Binding Site†

Douglas J. Scothorn, Walter E. Wojcicki, Eric J. Hustedt, Albert H. Beth, and Charles E. Cobb*

Department of Molecular Physiology and Biophysics, Vanderbilt University, Nashville, Tennessee 37232-0615

Received January 22, 1996; Revised Manuscript Received March 25, 1996⊗

ABSTRACT: A new spin-labeled maleimide derivative of the anion exchange inhibitor 4,4′-diaminodihydrostilbene-2,2′-disulfonate (H_2DADS) has been synthesized as a site-specific molecular probe of the stilbenedisulfonate binding site of the anion exchange protein 1 (AE-1; band 3) in human erythrocytes. This probe, SL-H_2DADS-maleimide, specifically and covalently labels the M_r 17 kDa integral membrane segment of band 3 with a 1:1 stoichiometry and inhibits essentially 100% of the band 3-mediated anion exchange. The linear V_1 EPR spectrum of spin-labeled intact erythrocytes is indicative of a spatially isolated probe which is effectively immobilized on the submicrosecond time scale. Several independent lines of experimental evidence have shown that the nitroxide moiety of SL-H_2DADS-maleimide-labeled band 3 is sequestered in a highly protected protein environment. These results are consistent with the observation that the spin-label is rigidly linked to band 3 in a fixed orientation with respect to the membrane normal axis [Hustedt, E. J., & Beth, A. H., (1996) *Biochemistry 35*, 6944−6954]. The nitroxide moieties of the SL-H_2DADS-maleimide-labeled band 3 dimer are greater than 20 Å from each other and are also more than 20 Å from a monomer−monomer contact surface defined by cross-linking with the spin-labeled reagent BSSDA [bis(sulfo-*N*-succinimidyl)doxyl-2-spiro-5′-azelate]. These properties make SL-H_2DADS-maleimide an extremely useful molecular probe for characterization of the physical properties of the band 3 stilbenedisulfonate binding site, determination of distances between the stilbenedisulfonate site and other segments of band 3, and investigation of the global rotational dynamics of human erythrocyte band 3.

The anion exchange protein of the human erythrocyte membrane, band 3, is responsible for the physiologically important one-for-one exchange of chloride and bicarbonate ions across the cell membrane [see Knauf (1979), Passow (1986), Jay and Cantley (1986), and Jennings (1984, 1989) for reviews]. Band 3 is a 911-amino acid integral membrane glycoprotein (Tanner et al., 1988; Lux et al., 1989) which consists of two structurally and functionally distinct domains. The anion transport function of band 3 is mediated through the 55K integral membrane domain,[1] which has a high α-helical content (Oikawa et al., 1985) and consists of an even number of membrane-spanning helices (between 10 and 16) traversing the bilayer (Lieberman & Reithmeier, 1988; Reithmeier, 1993; Wang et al., 1994). The remainder of the protein forms an elongated 43K hydrophilic cytoplasmic domain (Weinstein et al., 1978; Appell & Low, 1981) which is capable of binding to the erythrocyte cytoskeleton via ankyrin (band 2.1) and band 4.2 and contains binding sites for other intracellular proteins, including band 4.1, hemoglobin, aldolase, and glyceraldehyde-3-phosphate dehydrogenase [reviewed in Low (1986)]. The cytoplasmic domain does not appear to play a major role in band 3-mediated anion transport. Although the issue of the oligomeric state(s) of band 3 *in situ* is still incompletely resolved, there is an impressive accumulation of chemical cross-linking evidence demonstrating that the dimer is the most abundant form in both the erythrocyte membrane (Staros & Kakkad, 1983) and detergent-solubilized systems (Casey & Reithmeier, 1993). Many other studies, including radiation inactivation measurements (Cuppoletti et al., 1985) and size exclusion HPLC of detergent-solubilized band 3 (Casey & Reithmeier, 1991), also support dimeric band 3 as being the predominant form in the erythrocyte membrane.

As with the majority of other integral membrane proteins, the inherent difficulties in obtaining high-resolution structural data of band 3 have resulted in many important structural and dynamic questions remaining unanswered. The relative abundance of band 3 in the erythrocyte membrane (approximately 25% of the total membrane protein by weight) has made it an extremely important system for studying membrane protein structure−function relationships, since it can be readily studied in its native membrane. In addition, band 3 has been studied in reconstituted (Lukacovic et al., 1981) and solubilized systems (Casey & Reithmeier, 1991), and wild type (Groves & Tanner, 1994; Casey & Kopito, 1995) and site-directed mutants of band 3 (Garcia & Lodish, 1989; Sekler et al., 1995; Timmer et al., 1995) have been studied in various expression systems. A variety of proteolysis, covalent modification, and antibody binding studies have provided insights into the topology of the protein in

† Supported by Grants HL34737, RR04075, T32DK07186, and T32GM07347 from the National Institutes of Health.

* Address correspondence to Charles E. Cobb, Department of Molecular Physiology and Biophysics, 727 Light Hall, Vanderbilt University, Nashville, TN 37232-0615.

⊗ Abstract published in *Advance ACS Abstracts,* May 1, 1996.

[1] The integral membrane protein segment of band 3 designated as 17K is produced by chymotrypsin treatment of intact erythrocytes (yielding an M_r 58 kDa membrane domain, residues 1−553, and an M_r 38 kDa membrane domain, residues 554−911) followed by mild trypsin treatment of the unsealed ghost membranes (yielding an M_r 43 kDa soluble cytoplasmic domain, residues 1−359, and the M_r 17 kDa integral membrane peptide, residues 360−553, from the M_r 58 kDa membrane domain).

S0006-2960(96)00150-X CCC: $12.00

the membrane [reviewed in Jay and Cantley (1986) and Jennings (1984, 1989)]. Two-dimensional crystals of the integral membrane domain of band 3 have recently been prepared, and the contour of the dimer has been elucidated from electron microscopy data (Wang et al., 1993, 1994). Collectively, these studies have suggested possible locations for the functionally significant stilbenedisulfonate binding sites on each monomer; however, conclusive definition of the spatial arrangement of these sites remains elusive.

Many previous studies of band 3 structure and dynamics have relied on spectroscopic measurements using extrinsic molecular probes [e.g. Cherry et al. (1976), Dix et al. (1979), Rao et al. (1979), Macara and Cantley (1981), Schnell et al. (1983), Beth et al. (1986), Kaufmann et al. (1986), Anjaneyulu et al. (1988, 1989), and Wojcicki and Beth (1993b)]. Typically, these probes are anionic molecules which bind to band 3 at a high-affinity site which is believed to be at or near the physiologically important anion binding site (Falke & Chan, 1986a,b). Among the most informative of these extrinsic probes are various derivatives of the stilbenedisulfonate class of anion exchange inhibitors. Clearly, localization of the stilbenedisulfonate site within the global structure of the band 3 dimer and elucidation of the mechanism by which these compounds inhibit anion exchange are important questions of contemporary interest.

Electron paramagnetic resonance (EPR)[2] spectroscopy, using nitroxide spin-labels as site-specific probes, is proving to be an extremely important tool for investigation of the structure of integral membrane proteins [reviewed in Hubbell and Altenbach (1994)]. However, no covalently reactive spin-labeled stilbenedisulfonate derivatives have been previously reported. Schnell et al. (1983) and Wojcicki and Beth (1993b) have reported syntheses of nonreactive spin-labeled stilbenedisulfonates which have been employed in studies of stilbenedisulfonate binding cooperativity under equilibrium conditions, as well as the conformation and spatial arrangement of the stilbenedisulfonate sites. However, due to their intermediate binding affinities, these probes were not optimal for detailed structural or dynamic studies. In the present study, we report the chemical synthesis of a new covalently reactive nitroxide spin-label, 4-maleimidyl-4′-[(2,2,5,5-tetramethyl-3-carbamoylpyrrolin-1-yl)oxy]dihydrostilbene-2,2′-disulfonate (SL-H_2DADS-maleimide).

The results presented in this paper show that this probe affinity labels the exofacial stilbenedisulfonate site of band 3 and that the reaction site is contained exclusively, within the limits of detection, within the integral membrane 17K peptide of band 3 which contains the covalent reaction sites for H_2-DIDS (Okubo et al., 1994) and eosin-5-maleimide (Cobb & Beth, 1990). The local environment of this probe, when covalently bound to band 3, has been characterized using a number of complementary EPR approaches, and these results suggest a model in which the nitroxide resides in a highly protected environment within the protein interior and held in a unique orientation relative to the protein. These results provide a physical rationale for previously reported observations which show that there is a strong coupling between the nitroxide of SL-H_2DADS-maleimide and the global rotational motions of band 3 (Hustedt & Beth, 1995).

By labeling the stilbenedisulfonate site with SL-H_2DADS-maleimide, followed by cross-linking of the band 3 dimer with a spin-labeled homolog of BS[3] (BSSDA; Anjaneyulu et al., 1989) at a monomer−monomer contact, one can infer that the stilbenedisulfonate sites adjacent to the nitroxide moieties are located at least 20 Å from the site of monomer−monomer cross-linking by BSSDA. This result is discussed in relation to the postulated locations of the stilbenedisulfonate sites within the global structure of the band 3 dimer (Wang et al., 1993, 1994). SL-H_2DADS-maleimide is shown to offer important advantages for mapping intra- and intermolecular distances within the functional dimer. These properties of SL-H_2DADS-maleimide make it an excellent probe for EPR studies of the rotational dynamics of band 3 and, hence, for gaining insight into the oligomeric species present and the mechanical properties of various protein−protein interactions through detailed analyses of ST-EPR line shapes (Hustedt & Beth, 1995). Portions of this work have been published as abstracts (Wojcicki & Beth, 1993a; Cobb et al., 1994; Scothorn & Beth, 1994; Scothorn et al., 1995).

EXPERIMENTAL PROCEDURES

General Procedures. Intact human erythrocytes were obtained from venous blood freshly drawn into heparinized Vacutainer tubes from normal volunteer subjects and immediately placed on ice. Five volumes of ice-cold isotonic buffer (113cit7.4) was added to the whole blood, and the erythrocytes were collected by centrifugation. The remaining plasma components and buffy coat were removed by aspiration following three suspension and centrifugation cycles with approximately 10 volumes of 113cit7.4 as described in detail in previous work (Wojcicki & Beth, 1993b). All preparative steps were performed at 0−4 °C unless otherwise indicated.

Synthesis of SL-H_2DADS-maleimide. The starting material, mono-SL-H_2DADS, was prepared from the disodium salt of H_2DADS and the anhydride of 2,2,5,5-tetramethyl-3-pyrrolin-1-yloxy-3-carboxylic acid exactly as described in previous work (Wojcicki & Beth, 1993b). The maleamic acid derivative was prepared by drying 50 mg of the disodium salt of mono-SL-H_2DADS in a 10 mL round bottom flask for 1 h at 90 °C under strong vacuum, followed by addition of 5 mL of DMF (dried over 3 Å molecular sieves) and 42 mg of maleic anhydride (5-fold molar excess). The reaction vessel was fitted with a $CaSO_4$ drying tube, and the mixture was stirred for 1 h at 50 °C and then stirred overnight at room temperature. DMF was removed on a rotary evaporator, yielding a yellow-orange semisolid, which was dissolved in 1 mL of methanol and applied to a preparative 20 × 20 cm silica TLC plate (1000 μm thick

[2] Abbreviations: BSA, bovine serum albumin; BS[3], bis(sulfo-*N*-succinimidyl)suberate; BSSDA, bis(sulfo-*N*-succinimidyl)doxyl-2-spiro-5′-azelate; $C_{12}E_8$, octa(ethylene glycol) mono-*n*-dodecyl ether; Cr(Malt)$_3$, chromium(III) maltolate; CrOx, chromium(III) oxalate; CuKTSM$_2$, (3-ethoxy-2-butyraldehyde)bis(N^4,N^4-dimethylthiosemicarbazonato)copper(II); DIDS, 4,4′-diisothiocyanostilbene-2,2′-disulfonate; DPH, 1,2-diphenylhydrazine; EMA, eosin-5-maleimide; EPR, electron paramagnetic resonance; H_2DADS, 4,4′-diaminodihydrostilbene-2,2′-disulfonate; H_2DIDS, 4,4′-diisothiocyanodihydrostilbene-2,2′-disulfonate; MADS, 4-maleimidyl-4′-acetamidostilbene-2,2′-disulfonate; mono-SL-H_2DADS, 4-amino-4′-[(2,2,5,5-tetramethyl-3-carbamoylpyrrolin-1-yl)oxy]dihydrostilbene-2,2′-disulfonate; SL-acid, 2,2,5,5-tetramethyl-3-pyrrolin-1-oxyl-3-carboxylic acid; SL-H_2DADS-maleimide, 4-maleimidyl-4′-[(2,2,5,5-tetramethyl-3-carbamoylpyrrolin-1-yl)oxy]dihydrostilbene-2,2′-disulfonate; [^{15}N,^{2}H$_{13}$]-SL-H_2DADS-maleimide, [^{15}N,^{2}H$_{13}$]-isotopically substituted SL-H_2DADS-maleimide; 113cit7.4, 113 mM sodium citrate at pH 7.4; 5P7.4, 5 mM sodium phosphate at pH 7.4.

stationary phase; Whatman PK5F). The plate was developed using a mobile phase of $CH_3OH/CHCl_3/NH_4OH$ (50:50:5). Following drying of the plate, two minor bands ($R_f \approx 0.1$ and 0.9) and one major band ($R_f \approx 0.4$) were observed upon UV illumination. The major band was scraped from the plate, and the silica particles were thoroughly suspended and washed three times with 2 volumes of methanol. The suspension was vacuum filtered through a 0.45 μm nylon filter, yielding a pale yellow solution. Removal of methanol under reduced pressure afforded a yellow semisolid which was dissolved in 2 mL of deionized water and passed over a 0.5 × 2 cm column of BioRad AG-50W-X8 ion exchange resin (Na^+ form). The yellow eluent from the column was collected and lyophilized to dryness, yielding a fluffy pale yellow solid (78% yield). Analytical silica gel TLC (same mobile phase as described for purification above) showed a single spot ($R_f \approx 0.4$) with no trace of the mono-SL-H_2-DADS starting material ($R_f \approx 0.6$).

Ring closure to produce the maleimide derivative was accomplished by dissolving 45 mg of the maleamic acid derivative in 5 mL of acetic anhydride in a 10 mL round bottom flask followed by addition of 10 mg of anhydrous sodium acetate. The flask was fitted with a $CaSO_4$ drying tube and covered with aluminum foil, and the mixture was left stirring at room temperature for 8 days. The acetic anhydride was then removed under reduced pressure, yielding a yellow solid. The solid was dissolved in 1 mL of dry DMF and applied to a preparative silica gel TLC plate, and the plate was developed with DMF/$CHCl_3$ (50:50). The dense band ($R_f \approx 0.7$) observed upon UV illumination was scraped from the plate, and the material was solubilized from the silica by three thorough suspension and wash cycles with 2 volumes of dry DMF, which was vacuum filtered (0.45 μm nylon filter), and the DMF removed under reduced pressure, yielding a yellow solid. Analytical TLC (50:50 DMF/$CHCl_3$) gave a single spot upon UV illumination ($R_f \approx 0.7$) which was well-separated from the maleamic acid starting material ($R_f \approx 0.2$). On the basis of dry weight, the product obtained (64% yield) contained 0.97 spin/mol as determined by numerical double integration of the linear V_1 EPR spectrum and comparison with a standard solution of 2,2,5,5-tetramethylpyrrolin-1-yloxy-3-carboxylic acid (Kodak). Mass spectral analysis (FAB+) gave molecular ions at 664 $(M + H)^+$, 686 $(M + Na)^+$, and 642 mass units $(M + H - Na)^+$.

The [^{15}N,$^2H_{13}$]-SL-H_2DADS-maleimide derivative was prepared using these same procedures except that 2,2,5,5-tetramethyl-3-[1-^{15}N]pyrrolin-d_{13}-1-yloxy-3-carboxylic acid (MSD Isotopes) was employed to prepare the spin-label anhydride used in the first step of the reaction (Wojcicki & Beth, 1993b).

The SL-$^3H_2$DADS-maleimide derivative was prepared using the same procedures described above except 10 μCi of $^3H_2$DADS [custom tritiation of 4,4′-diaminostilbene-2,2′-disulfonate (DADS) performed by New England Nuclear] was added to 100 mg of the nonradioactive disodium salt of H_2DADS in the initial synthetic step.

Spin-Labeling of Band 3 in Intact Erythrocytes. Packed intact cells in 113cit7.4 were incubated with 30 μM [^{15}N,$^2H_{13}$]-SL-H_2DADS-maleimide (approximately 2-fold molar excess relative to the number of copies of band 3) for 45 min at room temperature. Ten volumes of 113cit7.4/0.5% BSA was then added, and the cells were incubated on ice for 10 min. Unreacted spin-label was removed from the labeled cells by suspension and centrifugation, first with 113cit7.4/0.5% BSA and then twice with 113cit7.4. Ghost membranes were prepared by lysis of spin-labeled intact erythrocytes via rapid dilution into 20 volumes of hypotonic buffer (5P7.4), followed by several suspension and centrifugation cycles until the ghost membranes appeared milky white (typically four to five washes).

DIDS Pretreatment. Pretreatment of packed erythrocytes with DIDS was accomplished by incubating washed erythrocytes with 100 μM DIDS (Sigma) in 113cit7.4 for 1 h at room temperature to allow sufficient time for all binding sites to be covalently blocked by DIDS (Cobb & Beth, 1990). Unreacted DIDS was removed by three suspension and centrifugation cycles, followed by incubation with 30 μM [^{15}N,$^2H_{13}$]-SL-H_2DADS-maleimide as described above.

Localization of the SL-H_2DADS-maleimide Reaction Site. Intact erythrocytes labeled with SL-$^3H_2$DADS-maleimide were incubated with 100 μg/mL TLCK-treated α-chymotrypsin (Sigma) at 37 °C for 30 min. Proteolytic digestion was stopped by two successive washing and centrifugation cycles with cold 113cit7.4 containing 30 μg/mL PMSF. Ghost membranes were prepared as described above, which were then treated with 10 μg/mL TPCK-treated trypsin (Sigma) for 30 min at room temperature to remove the 43K cytoplasmic domain of band 3. After trypsin treatment, the ghosts were washed once with 20 volumes of 5P7.4 containing 30 μg/mL PMSF, followed by two washes with 5P7.4. Ghost membrane proteins were separated on a 12% SDS−polyacrylamide gel (Laemmli, 1970). The SL-$^3H_2$-DADS-maleimide-labeled protein was localized by cutting one duplicate lane of the gel into 2 mm wide slices, soaking the slices in 1 mL of 5P7.4/100 mM NaCl/1% SDS overnight at room temperature, adding 5 mL of aqueous scintillation fluid, and liquid scintillation counting. The remaining lanes of the gel were stained with Coomassie Blue R-250 in order to visualize the peptides.

Collection of EPR Spectra. X-Band (~9.7 GHz) EPR spectra were collected on a Bruker ESP-300 spectrometer system equipped with an ER-042-MRH-E microwave bridge and an ER-4103-TM_{110} cavity. Sample temperature was controlled during data acquisition with an ER-4111-VT variable-temperature unit by blowing precooled compressed nitrogen gas through the front optical port. Spectra were accumulated with the ESP-300 data system by signal averaging (1024 data points per spectrum).

Packed intact erythrocytes or ghost membranes were loaded into either 50 μL disposable glass capillary tubes (Corning Pyrex disposable microsampling pipets) or TPX gas-permeable plastic capillary tubes (2 cm × 1mm inside diameter, 1.3 mm outside diameter, approximately 10 μL volume, a gift from Dr. J. B. Feix, National Biomedical ESR Center, Milwaukee, WI) and positioned in the temperature-controlled cavity. Linear V_1 EPR spectra were recorded at a 100 kHz field modulation with a 0.5 G amplitude (peak to peak, peroxylaminedisulfonate-calibrated; Beth et al., 1983) using a microwave observer power of 10 mW. EPR spectra of free spin-labels dissolved in various solvents (for determination of $\bar{a}$) were recorded at a 100 kHz field modulation and 0.2 G modulation amplitude with 1.0 mW microwave power.

CW power saturation EPR measurements were recorded at a 12.5 kHz field modulation and 0.5 G modulation amplitude over a range from 0.49 to 200 mW of microwave

power on spin-labeled ghost membranes loaded into TPX plastic capillary tubes.

Band 3 Functional Assay−Anion Exchange Rate Measurements. The anion exchange function of band 3 in intact cells was measured as radiolabeled sulfate uptake into chloride-loaded erythrocytes as previously described (Cobb & Beth, 1990).

Chemical Reduction of SL-H_2DADS-maleimide-Labeled Band 3. The accessibility of the nitroxide moiety of [^{15}N,$^{2}H_{13}$]-SL-H_2DADS-maleimide-labeled band 3 to chemical reducing agents was determined by quantitation of the signal loss as determined by double integration of the linear V_1 EPR signal following treatment of the labeled erythrocytes with either 10 mM sodium ascorbate or 1 mM DPH for 30 min at room temperature. The chemical reduction of the spin-label was determined in intact erythrocytes, erythrocyte ghost membranes, and ghost membranes solubilized with either 1% $C_{12}E_8$ or 1% SDS by double integration of the first derivative EPR spectra. Reduction of spin-label with DPH in intact erythrocytes was not quantitated due to the high degree of hemolysis which occurred with this agent.

CW Power Saturation Measurements of SL-H_2DADS-maleimide-Labeled Band 3. Ghost membranes from [^{15}N,$^{2}H_{13}$]-SL-H_2DADS-maleimide-labeled intact erythrocytes were washed twice with 40 volumes of 113cit7.4 to allow for tighter packing (resulting in an approximate 2-fold increase in signal amplitude). CW power saturation measurements were performed by blowing prepurified 99.95% compressed N_2, air (~21% O_2), or 95% O_2 gas through the front optical port of the EPR cavity. The samples were allowed to equilibrate with each gas for 15 min prior to collection of EPR spectra (Popp & Hyde, 1981).

The exogenous spin exchange agents CrOx (Altenbach et al., 1989a), Cr(Malt)$_3$ (Burchfield et al., 1994), and CuKTSM$_2$ (Subczynski et al., 1987, 1990) were added to the labeled ghosts prior to loading of the samples into the TPX capillary tubes. Cr(Malt)$_3$ was a gift from Dr. Gareth Eaton (University of Denver, Denver, CO). CuKTSM$_2$ was synthesized according to procedures described by Petering and coworkers (Petering et al., 1964; Van Giessen & Petering, 1968). Stock solutions of 50 mM CrOx (in 113cit7.4), 50 mM Cr(Malt)$_3$ (in 113cit7.4), and 10 mM CuKTSM$_2$ (in DMSO) were made immediately prior to use. CrOx- and Cr(Malt)$_3$-treated ghosts were prepared by adding 1 volume of the exchange agent stock solution to 4 volumes of labeled ghosts to give a 10 mM final concentration of the exchange agent. Treatment of the labeled ghosts with CuKTSM$_2$ required that the CuKTSM$_2$ stock solution in DMSO be added to a microfuge tube, followed by carefully layering an equal volume of the labeled ghosts onto the bright pink stock solution. Over the course of 1 h, the CuKTSM$_2$ equilibrated into the ghost membranes as shown by the appearance of a characteristic pink color in the ghost membrane layer. An aliquot was removed from the ghost layer and washed four times with 10 volumes of 113cit7.4, during which the pink color remained exclusively in the membrane phase. The presence of CuKTSM$_2$ in the ghost membranes was also confirmed by collecting an EPR signal of the paramagnetic copper(II) complex and comparing it with previously published spectra (Subczynski et al., 1987, 1990). In addition, the environmental specificity of these three agents was confirmed by CW power saturation studies on ghost membranes labeled with the spin-labeled fatty acid probe 16-doxylstearic acid and on BSA labeled with SL-H_2DADS-maleimide.

Linear V_1 EPR spectra were analyzed by plotting the amplitude of the low-field resonance line (ΔY) as a function of the square root of the incident power ($P^{1/2}$) as described by Altenbach et al. (1989a, 1994):

$$\Delta Y = \frac{IP^{1/2}}{\left[1 + \frac{(2^{1/\epsilon} - 1)P}{P_{1/2}}\right]^{\epsilon}} \quad (1)$$

where P is the incident microwave power, ϵ is a line shape adjustment parameter which has been shown to be unity for $\tau_R \geq 1$ μs (Haas et al., 1993), and I is a scaling factor. The parameter $P_{1/2}$ is defined as the microwave power at which the signal amplitude is one-half of the amplitude which it would be in the absence of saturation effects. The collision frequency (ω_e) is proportional to $\Delta P_{1/2}$, the difference between the values of $P_{1/2}$ determined in the presence and absence of a given paramagnetic agent (Altenbach et al., 1989a).

Determination of the Nitroxide Environment Polarity of SL-H_2DADS-maleimide-Labeled Band 3. The dependence of the hyperfine interactions of [^{15}N,$^{2}H_{13}$]-SL-H_2DADS-maleimide on the polarity and hydrophobicity of the environment was determined by comparing the isotropic coupling constants ($\bar{a}$) of [^{15}N,$^{2}H_{13}$]-SL-H_2DADS-maleimide either reacted with band 3 or dissolved in 113cit7.4 with a set of $\bar{a}$ values of the nitroxide spin-label acid precursor (SL-acid) of SL-H_2DADS-maleimide in solvents of differing polarity. Approximately 50 μg of SL-acid was dissolved in 1 mL of each of the solvents listed in Table 3. Oxygen was purged from the solutions by bubbling 99.95% nitrogen gas through the samples for 10 min. Values for $\bar{a}$ of SL-acid and [^{15}N,$^{2}H_{13}$]-SL-H_2DADS-maleimide dissolved in buffer were determined by measuring the separation, in Gauss, of the two motionally narrowed lines in the EPR spectrum. The values of A_{xx}, A_{yy}, and A_{zz} for [^{15}N,$^{2}H_{13}$]-SL-H_2DADS-maleimide-labeled band 3 were obtained from nonlinear least squares analysis of the linear EPR spectrum (Hustedt et al., 1993). The value of $\bar{a}$ was then calculated as $\bar{a} = {}^1/_3(A_{xx} + A_{yy} + A_{zz})$.

Due to the differences between the ^{14}N and ^{15}N gyromagnetic ratios, $\bar{a}$ values obtained for the isotopically substituted [^{15}N,$^{2}H_{13}$]-SL-H_2DADS-maleimide were converted into their [^{14}N]nitroxide equivalent:

$$\bar{a}(^{14}\mathrm{N}) = \bar{a}(^{15}\mathrm{N}) \times \frac{\gamma_n(^{14}\mathrm{N})}{\gamma_n(^{15}\mathrm{N})} = \bar{a}(^{15}\mathrm{N}) \times 0.7131 \quad (2)$$

where $\gamma_n(^{14}\mathrm{N})$ and $\gamma_n(^{15}\mathrm{N})$ are the nuclear gyromagnetic ratios for the ^{14}N and ^{15}N nuclei, respectively.

[^{15}N,$^{2}H_{13}$]-SL-H_2DADS-maleimide/[^{14}N,^{1}H]-BSSDA Double Labeling. Intact erythrocytes were labeled with 30 μM [^{15}N,$^{2}H_{13}$]-SL-H_2DADS-maleimide as described above. The labeled band 3 was cross-linked into covalent dimers with 2 mM ^{14}N-BSSDA (Anjaneyulu et al., 1989), followed by preparation of ghost membranes as described above. The labeled ghost membranes were stripped of cytoplasmic proteins by incubation with 2 mM EDTA (pH 12) for 15 min. The stripped ghosts were then pelleted by centrifugation and washed twice in 5P7.4. An aliquot of the ghosts

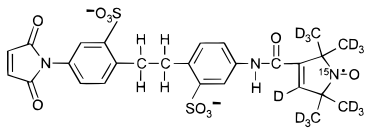

FIGURE 1: Chemical structure of [^{15}N,^{2}H$_{13}$]-SL-H$_2$DADS-maleimide.

was extracted with an equal volume of 2% $C_{12}E_8$ (w:v) in 5P7.4; insoluble material was removed by centrifugation, and the supernatant was collected for use in EPR studies.

In order to perform spectral subtractions on the composite spectrum collected on doubly labeled ghost membranes, several control samples were prepared and treated in the same manner as the doubly labeled ghosts. The spectrum of ^{14}N-BSSDA nonspecifically reacted with lipids was collected by prelabeling intact erythrocytes with 50 μM MADS followed by labeling with 50 μM ^{14}N-BSSDA. The spectrum of band 3 cross-linked to covalent dimers by ^{14}N-BSSDA was collected by prelabeling intact erythrocytes with 50 μM MADS, followed by labeling with 2 mM ^{14}N-BSSDA.

The degree of cross-linking by either BSSDA or BS^3 was assessed by SDS−PAGE (Fairbanks et al., 1971). The conversion of monomeric band 3 to dimeric band 3 was determined by densitometric analysis of the Coomassie Blue-stained band corresponding to monomeric band 3 using the Collage program (Fotodyne, Inc.) on a Macintosh computer.

RESULTS

Characterization of Spin-Label Reaction with the Stilbenedisulfonate Site. The V_1 linear EPR spectrum of [^{15}N,^{2}H$_{13}$]-SL-H$_2$DADS-maleimide (chemical structure shown in Figure 1) dissolved in 113cit7.4 buffer is shown in Figure 2A. The sharp two-line spectrum is characteristic of an [^{15}N]-nitroxide freely tumbling in solution. The V_1 linear EPR spectrum of [^{15}N,^{2}H$_{13}$]-SL-H$_2$DADS-maleimide-labeled intact erythrocytes at 20 °C is shown in Figure 2B. This spectrum is characteristic of a highly immobilized ($\tau_r \geq 1$ μs) and spatially isolated [^{15}N]nitroxide spin-label. In addition, the signal amplitude (double integral) of this spectrum indicates a spin-label concentration consistent with the estimated concentration of band 3 monomers present in packed intact erythrocytes ($\sim$15 μM; Wojcicki, 1993). In addition to the immobilized signal, a very small (<2% of the total integrated signal intensity) partially immobilized signal is observed which can be attributed to the presence of some nonspecific reaction of spin-label with other membrane components, the most likely candidate being membrane aminophospholipids.

The specificity of SL-H$_2$DADS-maleimide was verified by examining spin-label reaction following pretreatment of band 3 exofacial binding sites by the specific irreversible anion exchange inhibitor DIDS. The spectrum of DIDS-pretreated erythrocytes in Figure 2C shows reduction of the total EPR signal by 98%, i.e. complete blockage of the highly immobilized, spatially isolated [^{15}N]nitroxide spin-label, thus verifying the specificity of SL-H$_2$DADS-maleimide reaction for the stilbenedisulfonate site of band 3. Likewise, prelabeling of intact erythrocytes with EMA, a commonly employed band 3 optical probe, inhibits subsequent specific labeling with SL-H$_2$DADS-maleimide by greater than 95% (data not shown). Neither DIDS nor EMA significantly inhibits nonspecific labeling of aminophospholipid head groups. In addition, prelabeling of intact erythrocytes with

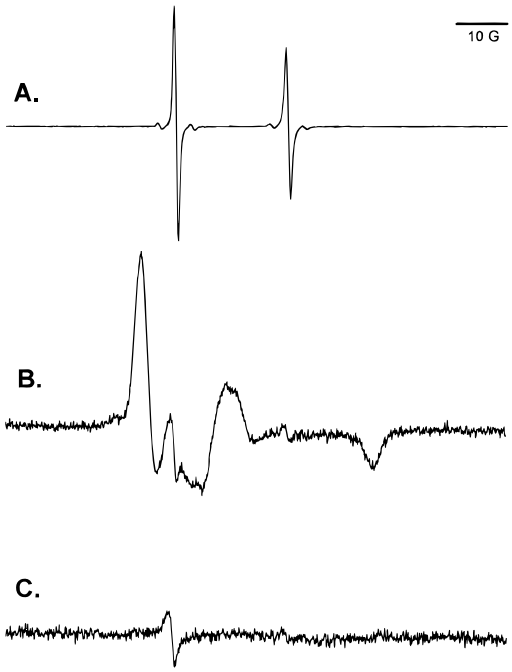

FIGURE 2: Linear V_1 EPR spectra of [^{15}N,^{2}H$_{13}$]-SL-H$_2$DADS-maleimide in solution and reacted with erythrocytes. Spectrum A was recorded on [^{15}N,^{2}H$_{13}$]-SL-H$_2$DADS-maleimide dissolved in 113cit7.4. Spectrum B was recorded on intact erythrocytes labeled with 30 μM [^{15}N,^{2}H$_{13}$]-SL-H$_2$DADS-maleimide. Spectrum C was recorded on intact erythrocytes prelabeled with DIDS, which is known to specifically block the exofacial stilbenedisulfonate binding site, followed by labeling with 30 μM [^{15}N,^{2}H$_{13}$]-SL-H$_2$DADS-maleimide. The DIDS-pretreated spectrum only contains a very small fast motion EPR signal arising from a small amount of nonspecific reaction of SL-H$_2$DADS-maleimide. By double integration of each spectrum, it was found that the nonspecific component contributed only 1.9% to the total V_1 absorption signal of the control-labeled erythrocytes (spectrum B).

SL-H$_2$DADS-maleimide inhibits subsequent reaction with EMA by greater than 95% (data not shown). These results are consistent with those of Cobb and Beth (1990), who showed that the EMA reaction site and the reaction sites of the stilbenedisulfonates DIDS and H$_2$DIDS are mutually exclusive.

Reaction Site of SL-H$_2$DADS-maleimide. In nonproteolyzed erythrocyte membranes, more than 95% of the SL-^{3}H$_2$DADS-maleimide is localized in a single diffuse band on SDS−PAGE which corresponds to the intact band 3 monomer (Figure 3B). Following chymotrypsin treatment of intact erythrocytes and trypsin treatment of ghost membranes, greater than 95% of the SL-^{3}H$_2$DADS-maleimide is found in a sharp SDS−PAGE band corresponding to the 17K integral membrane segment of band 3 (Figure 3C). This is the same proteolytic fragment of band 3 with which EMA (Lys-430; Cobb & Beth, 1990) and H$_2$DIDS at neutral pH (Lys-539; Okubo et al., 1994) have been shown to react.

Anion Exchange Studies. Functional assays were performed to determine if SL-H$_2$DADS-maleimide-labeled chloride-loaded erythrocytes could transport sulfate via band 3-mediated anion exchange. The results of this functional assay are shown in Figure 4. The sulfate uptake data clearly show that labeling erythrocytes with SL-H$_2$DADS-maleimide (solid circles), at a concentration of 1 mol of spin-label per mole of band 3 monomer completely inhibits sulfate−chloride exchange (open circles, control erythrocyte anion exchange). This result is characteristic of the inhibition of

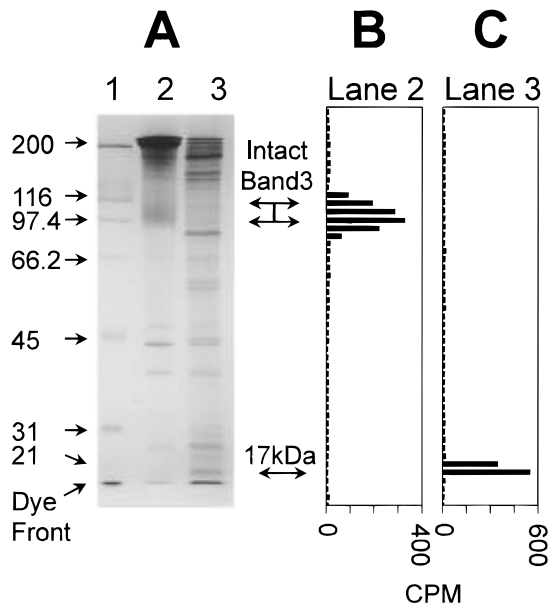

FIGURE 3: SDS−PAGE separation of control and chymotrypsin/trypsin-cleaved ghost membranes labeled with SL-$^3H_2$DADS-maleimide. Ghost membrane proteins were separated by SDS−PAGE (Laemmli, 1970). Protein bands visualized by staining with Coomassie Blue R-250 are displayed in panel A for the following samples: lane 1, molecular weight standards; lane 2, control SL-H_2DADS-maleimide-labeled membranes; and lane 3, chymotrypsin/trypsin-treated SL-H_2DADS-maleimide-labeled membranes. The radioactivity profiles shown in panels B and C (control and chymotrypsin/trypsin-treated membranes, respectively) were obtained by slicing duplicate lanes of the same gel before staining with Coomassie Blue and liquid scintillation counting of the slices.

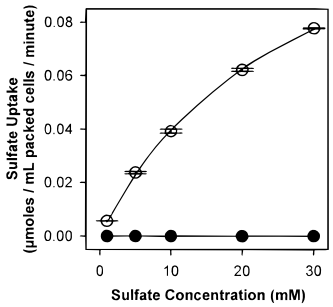

FIGURE 4: Sulfate transport by band 3. The uptake of radioactive sulfate ion ($^{35}SO_4^{2-}$) into chloride-loaded erythrocytes was measured (Cobb & Beth, 1990). The K_m and V_{max} for sulfate exchange with chloride, calculated by fitting the Michaelis−Menten equation to the data, for control cells (○) were 27.0 ± 1.4 mM and 0.147 ± 0.004 μmol of sulfate (mL of packed cells)$^{-1}$ min^{-1}, respectively. Labeling of erythrocytes with SL-H_2DADS-maleimide (●) essentially completely inhibited sulfate/chloride exchange (>99%).

band 3-mediated anion exchange by the stilbenedisulfonate class of inhibitors, including DIDS and H_2DIDS.

Local Environment of the Nitroxide Moiety of SL-H_2DADS-maleimide. Three complementary EPR approaches have been utilized to characterize the local environment of the nitroxide moiety of SL-H_2DADS-maleimide-labeled band 3. Chemical reduction studies and CW power saturation studies both address the accessibility of the nitroxide to agents which partition preferentially into either the aqueous or lipid environments. These studies seek to define the degree of exposure of the distal portion of the stilbenedisulfonate site, defined by the nitroxide moiety of SL-H_2DADS-maleimide, to the extracellular water, intracellular water, membrane lipids, and protein interior. Measurement of the hyperfine

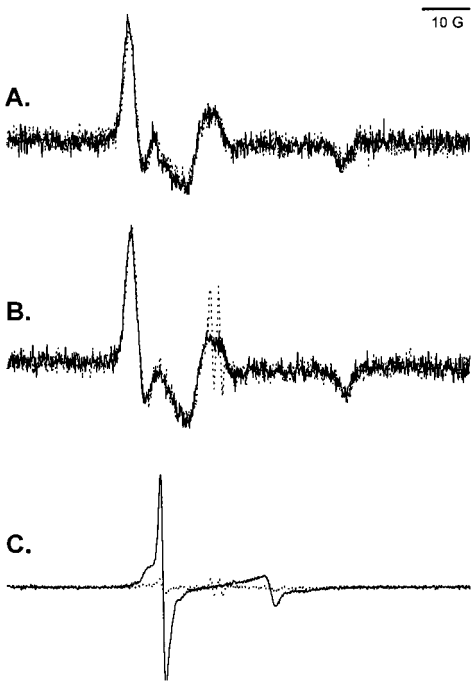

FIGURE 5: Chemical reduction of [^{15}N,$^2H_{13}$]-SL-H_2DADS-maleimide-labeled band 3. The spectra overlaid in panel A were recorded on control SL-H_2DADS-maleimide-labeled ghost membranes (solid line) and SL-H_2DADS-maleimide-labeled ghost membranes treated with 1 mM DPH for 30 min at 20 °C (dotted line). Displayed in panel B are spectra recorded on control SL-H_2DADS-maleimide-labeled ghost membranes (solid line) and SL-H_2DADS-maleimide-labeled ghost membranes treated with 10 mM sodium ascorbate for 30 min at 20 °C (dotted line). Panel C shows that solubilization of the SL-H_2DADS-maleimide-labeled ghost membranes with 1% SDS significantly alters the linear V_1 EPR spectrum (solid line), indicating extensive disruption of the native tertiary structure of band 3. Treatment of this SDS-solubilized sample with 10 mM sodium ascorbate for 30 min at 20 °C chemically reduced <90% of the SL-H_2DADS-maleimide-labeled band 3 (dotted line). The sharp doublets in the center of the spectra in panels B and C arise from the presence of a transient ascorbyl radical.

coupling constant ($\bar{a}$) of the nitroxide moiety of SL-H_2-DADS-maleimide has allowed the polarity and hydrogen-bonding character of the nitroxide environment to be determined. These latter studies address the question of whether hydrogen bonding between the nitroxide and band 3 occurs, an interaction which should complement the covalent bond and other probe affinity interactions for coupling the motions of the spin-label moiety to that of the protein.

In the chemical reduction studies, the nitroxide moiety of [^{15}N,$^2H_{13}$]-SL-H_2DADS-maleimide-labeled band 3 was not reduced by either the water-soluble reducing agent, sodium ascorbate, or the lipid-soluble reducing agent, DPH, under conditions where the native conformation of band 3 was preserved (intact erythrocytes, ghost membranes, and $C_{12}E_8$-solubilized ghost membranes). Under each of these conditions, greater than 95% of the EPR signal remained after 30 min of exposure to the reducing agent (Figure 5, Table 1). The V_1 EPR spectra of [^{15}N,$^2H_{13}$]-SL-H_2DADS-maleimide-labeled band 3 in intact erythrocytes, ghost membranes, and $C_{12}E_8$-solubilized ghost membranes are indistinguishable from one another, and the nitroxide moieties are identically resistant to chemical reduction by either sodium ascorbate or DPH. This finding is consistent with previous studies (Lieberman & Reithmeier, 1983; Casey & Reithmeier, 1991)

Table 1: Reduction of the Nitroxide Moiety of [^{15}N,^{2}H$_{13}$]-SL-H$_2$DADS-maleimide-Labeled Band 3 by Environment-Specific Chemical-Reducing Agents

	intact erythrocytes	erythrocyte ghosts	$C_{12}E_8$-solubilized ghosts	SDS−solubilized ghosts
sodium ascorbate	<2%	<2%	<2%	92%
DPH	ND[a]	<5%	<5%	96%

[a] Not determined due to a high degree of DPH-induced hemolysis of intact erythrocytes.

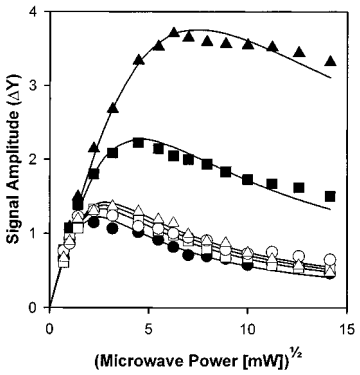

FIGURE 6: CW power saturation EPR measurements of [^{15}N,^{2}H$_{13}$]-SL-H$_2$DADS-maleimide-labeled ghost membranes. Control data (●) were collected in the presence of nitrogen gas only. Replacement of the nitrogen with either air (~21% oxygen, ■) or 100% oxygen (▲) resulted in a dose-dependent increase in the value of $\Delta P_{1/2}$. In contrast, neither the water-soluble spin exchange agents CrOx (□) or Cr(Malt)$_3$ (△) nor the lipid-soluble spin exchange agent CuKTSM$_2$ (○) showed any effect upon the value of $\Delta P_{1/2}$. The solid lines for each data set are fits to eq 1.

Table 2: CW Power Saturation Parameters for [^{15}N,^{2}H$_{13}$]-SL-H$_2$DADS-maleimide-Labeled Band 3 in the Presence of Various Environment-Specific Paramagnetic Exchange Agents

	$P_{1/2}$ (mW)	$\Delta P_{1/2}$ (mW)	relative collision frequency
nitrogen	6.0	−	
air (21% O$_2$)	20.8	14.8	+
100% oxygen	56.5	50.5	++
CrOx	7.1	1.1	−
Cr(Malt)$_3$	8.1	2.1	−
CuKTSM$_2$	7.6	1.6	−

Table 3: Values of the Hyperfine Coupling Constant, $\bar{a}$, for SL-acid Dissolved in Various Solvents of Differing Polarity and Hydrogen-Bonding Characteristics

solvent	solvent class	$\bar{a}$ (G)	solvent	solvent class	$\bar{a}$ (G)
n-hexane	NP	13.96	DMSO	P/NHB	14.61
cyclohexane	NP	14.02	isoamyl alcohol	P/HB	14.81
ethyl ether	P/NHB	14.14	2-propanol alcohol	P/HB	14.82
p-xylene	NP	14.16	band 3[a]		14.82
toluene	P/NHB	14.17	*n*-pentanol	P/HB	14.83
benzene	NP	14.18	*n*-propanol	P/HB	14.86
THF	P/NHB	14.20	isobutanol	P/HB	14.86
nitrobenzene	P/NHB	14.38	ethanol	P/HB	14.89
1,4-dioxane	P/NHB	14.43	methanol	P/HB	14.96
DMF	P/NHB	14.45	benzyl alcohol	P/HB	15.08
dichloromethane	P/NHB	14.45	formamide	P/HB	15.25
chloroform	P/NHB	14.53	water	P/HB	15.96
acetonitrile	P/NHB	14.57	113cit7.4[b]		15.99

[a] The value of $\bar{a}$ determined for [^{15}N,^{2}H$_{13}$]-SL-H$_2$DADS-maleimide-labeled band 3, on the basis of nonlinear least squares analysis, converted to the ^{14}N equivalent using eq 2. [b] The value of $\bar{a}$ determined for [^{15}N,^{2}H$_{13}$]-SL-H$_2$DADS-maleimide dissolved in 113cit7.4 converted to the ^{14}N equivalent using eq 2.

which have shown that solubilization of band 3 with $C_{12}E_8$ appears to maintain the native tertiary and quaternary structure of the protein. In ghost membranes prepared from labeled erythrocytes solubilized with SDS, which disrupts the native conformation of band 3, greater than 90% signal loss was observed upon treatment with sodium ascorbate (Figure 5, Table 1). The EPR signal was also stable in intact erythrocytes, indicating that the nitroxide moiety is not exposed to the intracellular aqueous compartment, which contains approximately 100 μM ascorbic acid (Melhorn, 1991). In contrast, the spin-label TEMPOL (4-hydroxy-TEMPO), which readily permeates the membrane, is rapidly reduced by intracellular ascorbate (data not shown).

In the CW power saturation EPR studies, the nitroxide moiety of [^{15}N,^{2}H$_{13}$]-SL-H$_2$DADS-maleimide-labeled band 3 shows a concentration-dependent increase in the collision frequency with O$_2$, as shown by the increase in the $P_{1/2}$ values from 99.95% N$_2$, to air (~21% O$_2$; $\Delta P_{1/2}$ = 14.8 mW), to 100% O$_2$ ($\Delta P_{1/2}$ = 50.5 mW). Utilization of the environment-specific spin exchange agents, anionic CrOx, neutral Cr(Malt)$_3$, and lipophilic CuKTSM$_2$, provides additional information about the local environment of the nitroxide. The nitroxide moiety of [^{15}N,^{2}H$_{13}$]-SL-H$_2$DADS-maleimide-labeled band 3 is protected from collision with both the water-soluble exchange agents, CrOx ($\Delta P_{1/2}$ = 1.1 mW) or Cr(Malt)$_3$ ($\Delta P_{1/2}$ = 2.1 mW), and the lipid-soluble exchange agent, CuKTSM$_2$ ($\Delta P_{1/2}$ = 1.6 mW) (Figure 6, Table 2). These results provide solid indications that the nitroxide moiety of [^{15}N,^{2}H$_{13}$]-SL-H$_2$DADS-maleimide-labeled band 3 is localized within a protected environment on band 3, which effectively shields the nitroxide from collisions with the bulky exchange agents, but which does allow collisional contact between molecular oxygen and the nitroxide in the protein interior. The use of both the anionic CrOx and the neutral Cr(Malt)$_3$ allowed for the effect of electrostatic interactions to be addressed in the accessibility of the nitroxide to collision with the water-soluble agents. Since both CrOx and Cr(Malt)$_3$ gave very similar $\Delta P_{1/2}$ values, the inaccessibility of the nitroxide to the aqueous environment is not due to charge repulsion effects between the anionic CrOx and the anionic stilbenedisulfonate. The lipophilic spin exchange agent CuKTSM$_2$ has not previously been utilized for nitroxide accessibility studies, but its partitioning properties appear to be superior to those reported for the more commonly used lipid-soluble agents nickel(II) EDDA and nickel(II) acetylacetonate (Altenbach et al., 1994). Further elaboration on the possible reason for these observations is presented in the Discussion.

The isotropic hyperfine coupling constant ($\bar{a}$) is extremely sensitive to the polarity and hydrogen-bonding character of the solvent environment (Gough, 1973; Griffith et al., 1974; Reddoch & Konishi, 1979). The spin-label precursor of SL-H$_2$DADS-maleimide (SL-acid) was dissolved in a number of solvents (Table 3), which were divided into three classes according to the scheme of Reddoch and Konishi (1979): nonpolar solvents (NP), polar non-hydrogen-bonding solvents (P/NHB), and hydrogen-bonding (HB) solvents. The value of $\bar{a}$ for SL-acid ranges from 13.96 G (in *n*-hexane) to 15.96 G (in water). For [^{15}N,^{2}H$_{13}$]-SL-H$_2$DADS-maleimide dissolved in 113cit7.4, $\bar{a}$ = 22.42 G; conversion to the [^{14}N]-nitroxide equivalent gives a value of $\bar{a}$ = 15.99 G. This value is essentially identical to that of SL-acid in water.

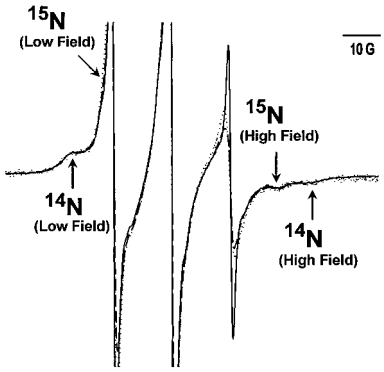

FIGURE 7: Linear V_1 EPR spectra of [^{15}N,^{2}H$_{13}$]-SL-H$_2$DADS-maleimide/[^{14}N,^{1}H]-BSSDA doubly labeled samples. Overlaid spectra recorded on intact erythrocytes (solid line), ghost membranes (dashed line), and a $C_{12}E_8$ extract of the labeled ghost membranes (dotted line). The amplitudes of the spectra have been magnified to better show the high-field and low-field spectral features of [^{14}N,^{1}H]-BSSDA immobilized on the EPR time scale and [^{15}N,^{2}H$_{13}$]-SL-H$_2$DADS-maleimide reacted at the stilbenedisulfonate site.

Computer fitting of the EPR spectrum of [^{15}N,^{2}H$_{13}$]-SL-H$_2$-DADS-maleimide-labeled band 3 at room temperature using a nonlinear least squares algorithm previously described by Hustedt et al. (1993) yields the following values: $A_{zz} = 46.17$ G, $A_{xx} = 7.98$ G, and $A_{yy} = 8.19$ G [see Figure 2 in Hustedt and Beth (1996)]; the fitting results in a value of $\bar{a} = 20.78$ G. Conversion to the [^{14}N]nitroxide equivalent, using eq 2, gives $\bar{a} = 14.82$ G, comparable to the values of $\bar{a}$ for SL-acid dissolved in isoamyl alcohol ($\bar{a} = 14.81$ G), *n*-pentanol ($\bar{a} = 14.82$ G), and 2-propanol ($\bar{a} = 14.83$ G). The most polar of the P/NHB solvents described by Reddoch and Konishi (1979) is DMSO, and the value of $\bar{a}$ for SL-acid dissolved in DMSO ($\bar{a} = 14.61$ G) is significantly smaller than that determined for SL-H$_2$DADS-maleimide-labeled band 3. The value of $\bar{a}$ for [^{15}N,^{2}H$_{13}$]-SL-H$_2$DADS-maleimide-labeled band 3 indicates a significantly more polar environment than any of the pure hydrocarbon solvents (which should mimic the middle regions of the lipid bilayer). The value of $\bar{a}$ for SL-H$_2$DADS-maleimide-labeled band 3 is in the range which occurs only for solvents capable of hydrogen bonding with the nitroxide. These data strongly suggest that the nitroxide moiety of SL-H$_2$DADS-maleimide is hydrogen-bonded to an amino acid side chain or the protein backbone (although it is also possible that the nitroxide hydrogen-bonding partner could be a water molecule sequestered in the SL-H$_2$DADS-maleimide binding pocket).

Distance Constraints for the Stilbenedisulfonate Site and a Monomer−Monomer Contact Surface in Band 3. Previous EPR studies have shown that the stilbenedisulfonate binding sites on adjacent monomers of band 3 are more than 20 Å apart (Wojcicki & Beth, 1993), a result which supports earlier studies using fluorescence resonance energy transfer (Macara & Cantley, 1981). However, the spatial arrangement of these sites relative to the monomer−monomer interface has not been resolved. The work of Staros and Kakkad (1983) and Jennings and Nicknish (1985) has shown that the bis(sulfo-*N*-succinimidyl) cross-linking reagents, including the prototypical analog BS^3, form an extracellular covalent cross-link between band 3 monomers. Anjaneyulu et al. (1989) subsequently demonstrated that BSSDA could likewise cross-link band 3 monomers, under similar conditions. Thus, the possibility exists for addressing the spatial arrangement of the stilbenedisulfonate sites, labeled with [^{15}N,^{2}H$_{13}$]-SL-H$_2$DADS-maleimide, and the monomer−monomer interface, cross-linked with ^{14}N-BSSDA, with a double-labeling experiment.

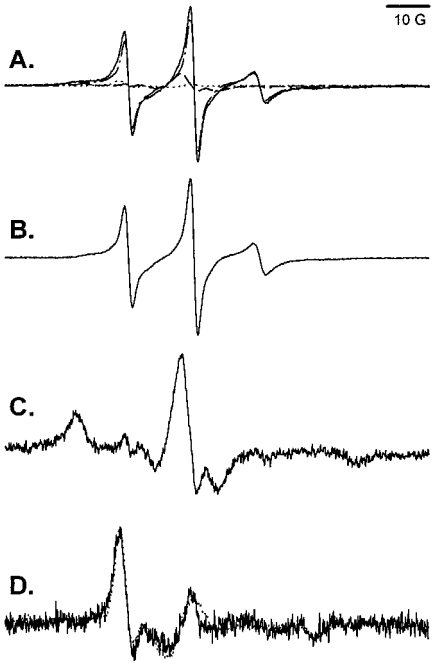

FIGURE 8: Deconvolution of the linear EPR spectrum of [^{15}N,^{2}H$_{13}$]-SL-H$_2$DADS-maleimide/[^{14}N,^{1}H]-BSSDA doubly labeled erythrocyte ghost membranes solubilized in $C_{12}E_8$. Panel A shows the linear V_1 EPR spectrum of [^{15}N,^{2}H$_{13}$]-SL-H$_2$DADS-maleimide/[^{14}N,^{1}H]-BSSDA doubly labeled erythrocyte ghost membrane $C_{12}E_8$-solubilized extract (solid line) with the three component spectra overlaid: [^{14}N,^{1}H]-BSSDA reacted with membrane lipids (dot−dash line), [^{14}N,^{1}H]-BSSDA immobilized on the EPR time scale (dashed line), and [^{15}N,^{2}H$_{13}$]-SL-H$_2$DADS-maleimide reacted at the stilbenedisulfonate site (dotted line). The [^{14}N,^{1}H]-BSSDA−lipid component is shown in panel B and contributes 66.4% of the total signal. The [^{14}N,^{1}H]-BSSDA−protein component is shown in panel C, which is at least partly derived from cross-linking of band 3 to covalent dimers, and contributes 27.4% of the total signal. The [^{15}N,^{2}H$_{13}$]-SL-H$_2$DADS-maleimide-labeled band 3 spectrum obtained by spectral subtractions as described in the text (solid line) is shown in panel D, and this spectrum makes up 6.2% of the total signal. For comparison purposes, the linear V_1 EPR spectrum of [^{15}N,^{2}H$_{13}$]-SL-H$_2$DADS-maleimide-labeled band 3 in non-cross-linked ghost membranes is overlaid (dotted line). Since these two spectra are clearly indistinguishable, there are no dipolar interactions between the nitroxide moieties of ^{14}N-BSSDA and [^{15}N,^{2}H$_{13}$]-SL-H$_2$DADS-maleimide.

The results of this double-labeling experiment are shown in Figures 7 and 8. Figure 7 shows a magnified view of the composite experimental spectra obtained from intact erythrocytes (solid line), ghost membranes (dashed line), and ghost membranes solubilized with $C_{12}E_8$ (dotted line). In these spectra, the distinct, sharp signal from [^{15}N,^{2}H$_{13}$]-SL-H$_2$-DADS-maleimide at the stilbenedisulfonate site can be readily identified in the high-field region of the spectra. In the low-field region of the spectra, the [^{15}N]nitroxide signal is obscured by the partially immobilized [^{14}N]nitroxide spectrum, which originates from nonspecific labeling of membrane aminophospholipids, and perhaps other membrane components, with BSSDA. The full EPR spectrum of [^{15}N,^{2}H$_{13}$]-SL-H$_2$DADS-maleimide-labeled band 3 can be obtained by spectral subtractions from the experimental composite spectrum.

Solubilization of the doubly labeled ghost membrane with the neutral detergent $C_{12}E_8$ results in a decrease in the line

width of the signal derived from BSSDA-labeled lipids, thereby facilitating spectral subtraction to obtain the three component spectra. Figure 8 shows the results of the spectral subtractions performed on solubilized doubly labeled erythrocyte ghost membranes. The upper spectrum (Figure 8A) shows the composite experimental spectrum (solid line), which is made up of three components: [^{15}N,^{2}H$_{13}$]-SL-H$_2$-DADS-maleimide reacted at the stilbenedisulfonate site (dotted line) which makes up 6.2% of the total signal; [^{14}N,^{1}H]-BSSDA immobilized on the EPR time scale which has been shown previously to arise, in part, from BSSDA involved in cross-linking of adjacent monomers (Anjaneyulu et al., 1989) (dashed line) contributing 27.4% of the total signal; and [^{14}N,^{1}H]-BSSDA reacted with membrane lipids (dot−dash line) which makes up 66.4% of the total signal. Three samples were prepared in order to carry out the spectral subtractions, as described in the Experimental Procedures. The line shape for [^{15}N,^{2}H$_{13}$]-SL-H$_2$DADS-maleimide reacted specifically at the stilbenedisulfonate site was obtained by labeling intact erythrocytes, followed by preparation of ghost membranes and solubilization of the ghost membranes in $C_{12}E_8$. The line shape for [^{14}N,^{1}H]-BSSDA reacted with lipid head groups was obtained by preblocking intact erythrocytes with MADS and then subsequently labeling with either 50 μM or 2 mM BSSDA. The low concentration of BSSDA results primarily in lipid head group labeling, as shown by the dominance of the partially immobilized three-line spectrum. The high concentration of BSSDA results in both the partially immobilized three-line spectrum and a significant broad signal arising from BSSDA-cross-linked band 3 and possibly other membrane components. These two components are resolved by subtracting the scaled EPR signal of the 2 mM BSSDA sample from that of the 50 μM BSSDA sample, with flat base lines in the extrema regions as the end point. This yields the partially immobilized three-line spectrum (Figure 8B). This difference spectrum is then subtracted from that of the 2 mM BSSDA sample, removing the small amount of partially immobilized component, to yield the broad, slow motion spectrum of BSSDA-cross-linked band 3 and other membrane components (Figure 8C). Finally, these two component spectra were then subtracted from the doubly labeled composite spectrum to yield the spectrum of [^{15}N,^{2}H$_{13}$]-SL-H$_2$DADS-maleimide labeled at the stilbenedisulfonate site (Figure 8D, solid line). It is apparent that this line shape is indistinguishable from the one obtained by labeling of intact erythrocytes with [^{15}N,^{2}H$_{13}$]-SL-H$_2$-DADS-maleimide without subsequent BSSDA cross-linking of band 3 (Figure 8D, dotted line). Thus, in the $C_{12}E_8$-solubilized system, where reasonably precise spectral subtractions are possible, there is no evidence for any spectral distortion due to dipole−dipole interaction between the two different nitrogen isotope spin-labels.

Integration of these three component signals indicated that approximately 4.4 mol of BSSDA reacted with protein per mole of SL-H$_2$DADS-maleimide. The expected ratio of BSSDA to SL-H$_2$DADS-maleimide would be 1:1 if a unique monomer−monomer cross-link site exists and the C_2 symmetry-related sites do not sterically interfere with one another. However, at the high concentration of BSSDA (2 mM) employed to drive cross-link formation to near completion, there is substantial nonspecific labeling of additional sites, which may, or may not, be at the monomer−monomer interface of band 3, and other membrane proteins, including glycophorin, may also be labeled (Jennings & Nicknish, 1985). SDS−PAGE has confirmed that approximately 85% of the band 3 monomers have been cross-linked by BSSDA under these reaction conditions (data not shown). This level of BSSDA-cross-linked product would be sufficient to perturb the nitroxide signal from [^{15}N,^{2}H$_{13}$]-SL-H$_2$DADS-maleimide at the stilbenedisulfonate site if the two isotopically distinct nitroxides are within 20 Å of one another (Wojcicki & Beth, 1993b). Therefore, the minimum distance between the nitroxide moieties of [^{15}N,^{2}H$_{13}$]-SL-H$_2$DADS-maleimide and ^{14}N-BSSDA must be greater than 20 Å.

DISCUSSION

Site-specific molecular probes, in combination with spectroscopic techniques such as EPR, fluorescence, and phosphorescence, have been used extensively over the past two decades to characterize a wide range of structural and dynamic properties of membrane proteins, including human erythrocyte band 3. The stilbenedisulfonate site of band 3 has been the focus of several such studies, due to its importance as an affinity binding site for a number of potent anion exchange inhibitors. The stilbenedisulfonates, including the prototypical inhibitor DIDS, are fluorescent when bound to band 3. As discussed further below, fluorescence studies have been carried out using covalent and noncovalent derivatives of the stilbenedisulfonate class of inhibitors to address the accessibility and spatial arrangement (Rao et al., 1979; Macara & Cantley, 1981) of these functionally important sites. To date, however, there have not been any spin-labeled stilbenedisulfonates reported which can react covalently with band 3 and serve as an EPR probe of local and global structure of the protein. It should be emphasized that rigorous interpretation of data from spin-label and optical molecular probes routinely requires determination of the specificity of the probe for a specific membrane protein versus other proteins present in a complex assembly, the uniqueness of the probe's reaction site, in terms of both a unique amino acid and a unique conformation within the protein structure, and the degree of motional freedom of the probe relative to the protein with which it has reacted.

In this work, the synthesis of a new spin-label probe for the band 3 protein of human erythrocytes is described. The data presented here and by Hustedt and Beth (1995, 1996) show that SL-H$_2$DADS-maleimide reacts with high specificity toward band 3 in intact erythrocytes, that the labeling is highly specific for the integral membrane 17K peptide produced by chymotrypsin cleavage of intact erythrocytes followed by mild trypsin cleavage of ghost membranes, that the spin-label moiety adopts a unique and measurable geometry relative to the membrane normal axis of the erythrocyte, and that large amplitude, independent probe motion relative to band 3 is minimal. These properties make this an ideal probe for a wide range of studies of band 3 structure and dynamics, as discussed in the following paragraphs.

While we have yet to demonstrate that SL-H$_2$DADS-maleimide reacts with a single amino acid residue on the 17K peptide, it is likely that it reacts with the same lysine, Lys-539, as H$_2$DIDS (Okubo et al., 1994). Preliminary efforts to sequence the reaction site have indicated that the probe has reacted with a residue on a peptide whose N-terminus is Ile-516. This result rules out Lys-430, the

reaction site for EMA (Cobb & Beth, 1990), and Cys-479, the only cysteine in the 17K peptide, as potential reaction sites. However, the labeled peptide does potentially contain Lys-542 as well as Lys-539 as possible reaction sites. Further work will be required to rigorously differentiate between these two potential reaction sites. Although in general maleimides are much more reactive with cysteine than lysine, apparently the maleimide of SL-H_2DADS-maleimide is held in the correct proximity and orientation to allow the covalent reaction to proceed with Lys-539 or Lys-542. A similar case is the previously mentioned reaction of EMA with Lys-430 of band 3 (Cobb & Beth, 1990) under the same mild reaction conditions (pH 7.4, room temperature).

Characterization of SL-H_2DADS-maleimide Reaction with Band 3. SL-H_2DADS-maleimide reacts with band 3 at a stoichiometry of one spin-label molecule per band 3 monomer. There are several significant pieces of evidence that together make a strong argument for its affinity labeling band 3 at the functionally relevant stilbenedisulfonate binding site. The first piece of evidence is that pretreatment of erythrocytes with DIDS completely blocks the subsequent binding and reaction of SL-H_2DADS-maleimide with band 3 (Figure 2). DIDS and its dihydro derivative H_2DIDS have been extensively used to study both the structure and the anion exchange function of band 3 and, in fact, were useful in originally identifying band 3 as the anion exchange protein of the erythrocyte membrane (Knauf & Rothstein, 1971). The second line of evidence is the finding that bound spin-label completely blocks anion transport, as evaluated by measuring the rate of uptake of radiolabeled sulfate ion into chloride-loaded erythrocytes (Figure 4). The third line of evidence is that the amino acid residue labeled by this reagent is on the same 17K peptide fragment which is labeled by EMA (Cobb & Beth, 1990) and H_2DIDS (Okubo et al., 1994). Finally, preliminary data have suggested that SL-H_2DADS-maleimide may react with the same amino acid as H_2DIDS (Okubo et al., 1994).

There are obvious advantages for analyzing EPR data from spin-labeled band 3 if one does not have to consider spectral contributions from minor labeling of secondary sites. Therefore, it is important to carefully quantitate the specificity of labeling. The data in Figure 3 shows that more than 95% of the radioactivity from SL-$^3H_2$DADS-maleimide-labeled intact erythrocytes was recovered from a single broad band on SDS−PAGE, which corresponds exactly with the Coomassie staining region from monomeric band 3. Following chymotrypsin cleavage of labeled intact cells, preparation of ghost membranes, and mild trypsin cleavage of the ghost membranes, more than 90% of the radioactivity from SL-$^3H_2$DADS-maleimide was recovered in a sharp band on SDS−PAGE corresponding to the integral membrane 17K peptide. While one might argue that 5−10% of the labeling was directed to secondary sites on band 3 or even on other proteins, this is very unlikely since there was no region of the SDS−PAGE gel following proteolysis which gave any radioactivity counts statistically above background, except for those in the sharp 17K band. If minor labeling of another protein occurred which was obscured by the broad band 3 monomer region of the gel, it is unlikely that proteolysis would cleave this unidentified protein such that it would comigrate with the 17K peptide. These findings strongly suggest that SL-H_2DADS-maleimide does react at a single site on band 3, the stilbenedisulfonate site, when intact erythrocytes are labeled near the stoichiometry of band 3 monomers present. Absolute verification of single site labeling awaits chemical sequencing of the labeled proteolytic peptide derived from the 17K band 3 peptide.

Orientation of the Nitroxide Moiety Relative to Band 3. Detailed analysis of spectroscopic data requires the probe to have a unique reaction site and adopt a unique orientation relative to the protein. Although uniqueness of the labeling site has been demonstrated for other molecular probes of band 3, such as EMA (Cobb & Beth, 1990) and H_2DIDS (Okubo et al., 1994), a unique labeling geometry for these probes has not yet been reported. The orientational uniqueness of SL-H_2DADS-maleimide covalently reacted with band 3 has been addressed in great detail by Hustedt and Beth (1995, 1996). It was determined that the *z*-axis of the nitroxide was tilted by approximately 37° from the membrane normal axis and that all spin-label present was oriented within a narrow range of angles centered about 37° by computer modeling of the EPR spectra obtained from [^{15}N,$^2H_{13}$]-SL-H_2DADS-maleimide-labeled band 3 in intact erythrocytes which were oriented by flow through an EPR flat cell. These results, combined with the narrow line width obtained in the V_1 EPR spectrum (Figure 2), indicate that the nitroxide moiety is rigidly held in a unique environment. Moreover, the finding that all band 3-reacted spin-labels adopt the same orientation is consistent with the stilbenedisulfonate sites being related by C_2 symmetry about the membrane normal axis, as predicted by the cross-linking studies of Staros and Kakkad (1983) and the low-resolution structure of Wang et al. (1994). On the basis of the reaction specificity and the finding of a unique orientation, it is reasonable to analyze subsequent EPR data from SL-H_2DADS-maleimide-labeled band 3 in terms of a single unique species with a defined labeling geometry.

Accessibility of the Stilbenedisulfonate Binding Site. SL-H_2DADS-maleimide labels band 3 to form a complex in which the nitroxide moiety is sequestered in an environment which is remarkably inaccessible to either water-soluble or lipid-soluble reducing or spin exchange agents (Figures 5 and 6). This environment is significantly less polar than water and significantly more polar than the acyl chain region of the lipid bilayer of the erythrocyte membrane. The $\bar{a}$ value determined from spin-labeled band 3 is suggestive of a hydrogen-bonding environment, which likely involves an amino acid side chain or the protein backbone (Table 3), or possibly a water molecule sequestered in the SL-H_2DADS-maleimide binding pocket.

It is useful to compare this result with data obtained from band 3 labeled with the optical probe EMA, whose binding appears to overlap with the stilbenedisulfonate site (Cobb & Beth, 1990). Previous optical studies (Macara et al., 1983) have suggested that EMA reacted with band 3 is inaccessible to the water-soluble quenching agent Cs^+ from the extracellular space and partially quenched by a static mechanism by Cs^+ from the cytoplasmic side of the membrane. These findings could be interpreted as arising from a major portion of EMA being located within the interior of band 3, possibly within the anion passageway through the membrane, as if it were partially "transported". This interpretation does not preclude the possibility that EMA acts as a noncompetitive inhibitor of Cl^- exchange (Knauf et al., 1993; Liu & Knauf, 1993) since the small Cl^- ion may still be able to bind to

positively charged residues within the exchange pathway.

The inaccessibility of water and lipid-soluble paramagnetic broadening agents, such as CrOx and $Cr(Malt)_3$, to the nitroxide moiety of SL-H_2DADS-maleimide-labeled band 3 (Figure 6) provides additional, complementary data to support the previous hypothesis (Rao et al., 1979; Macara et al., 1983) that at least a portion of the stilbenedisulfonate site is located deep within the protein interior. Recently, Landolt-Marticorena et al. (1995) have shown that H_2-DIDS covalently bound to band 3 is inaccessible to anti-H_2-DIDS antibodies even after extensive proteolysis of extramembraneous loops. These data have strongly suggested that a major portion of the H_2-DIDS binding site is "buried" within the transmembrane domain of band 3. At first glance, the inaccessibility to chemical-reducing agents (Figure 5) appears simply to lend further support to these previous studies on accessibility. However, the extreme inaccessibility to both water- and lipid-soluble chemical-reducing agents is quite unusual. Simply placing the nitroxide moiety in a cleft of band 3 into which water and relatively small reducing agents such as ascorbate could diffuse would be expected to result in a measurable reduction rate, particularly at the high (10 mM) ascorbate concentration used in these studies. This is supported by ascorbate reduction studies of SL-H_2DADS-maleimide and spin-labeled maleimide (MSL)-labeled bovine serum albumin, as well as MSL-labeled glyceraldehyde-3-phosphate dehydrogenase, where the nitroxide moiety is rigidly held by interactions with amino acid side chains but is still rapidly (less than 1 min) and completely reduced by 10 mM ascorbate (data not shown). The value of $\bar{a}$ (Table 3) also supports a model in which the nitroxide moiety is held in a polar nonaqueous hydrogen-bonding environment.

Collectively, the previous optical studies, the inaccessibility to H_2-DIDS antibodies, and the current EPR results provide a solid indication that at least a portion of the stilbenedisulfonate site is buried deep within the tertiary or quaternary structure of the band 3 dimer. It is likely, on the basis of the folding model of Wang et al. (1994), that both EMA and SL-H_2DADS-maleimide form covalent bonds with lysines (Lys-430 and possibly Lys-539, respectively) which are exposed to the extracellular space. Interestingly, such a model is suggested by stilbenedisulfonate binding studies which have indicated a two-step binding process involving a rapid phase followed by a slower phase where the probe is "locked" in place (Dix et al., 1979). Given the length of the lysine side chain and the sizes of these molecular probes, it is reasonable to speculate that their distal ends extend into the anion passageway through the membrane, which effectively occludes at least a portion of these two spectroscopic probes from the intracellular and extracellular aqueous compartments. Since the lipid-soluble chemical reductant, DPH, and the lipid-soluble paramagnetic broadening agent, $CuKTSM_2$, are essentially incapable of colliding with the spin-label, it appears that the binding site is contained within the proteinaceous core of band 3 and therefore effectively insulated from the lipid bilayer. This model will be further discussed in relation to the known low-resolution structure of the band 3 dimer (Wang et al., 1993, 1994) below.

Insights into the Spatial Separation of the Stilbenedisulfonate Sites. The spatial separation of the stilbenedisulfonate sites, their disposition with respect to the interface between monomers, and their location within the known global structure of the band 3 dimer remain to be precisely defined. Previous fluorescence resonance energy transfer studies by Macara and Cantley (1981) and EPR studies by Wojcicki and Beth (1993a) have indicated that the stilbenedisulfonate sites are separated lengthwise by at least 20 Å and possibly by as much as 52 Å in the native dimer. These distances are consistent with the current studies which indicate that the nitroxide moieties of SL-H_2DADS-maleimide on adjacent monomers are at least 20 Å apart since no evidence of dipolar coupling is observed (Figure 2). Electron image analyses of two-dimensional crystals of the transmembrane domain of band 3 (Wang et al., 1993, 1994) have provided direct evidence that the dimer of band 3 exhibits C_2 symmetry around a central extracellular projection, a portion of which must be bisected by the monomer−monomer interface. Membrane impermeant cross-linking reagents, including BS^3 (Staros & Kakkad, 1983) and its spin-labeled homologue, BSSDA (Anjaneyulu et al., 1989), cross-link band 3 monomers by spanning the monomer−monomer interface at the extracellular surface. Given the similarities in covalent dimer formation as a function of concentration of the cross-linker, combined with the structural similarity of these two reagents, it is likely that they cross-link the same amino acids on the two interacting monomers. Jennings and Nicknish (1985) have shown that for BS^3 one end of this intersubunit cross-link involves either Lys-551 or Lys-562. In the folding model of Wang et al. (1994), these two Lys residues are predicted to be on an extracellular loop of band 3 between membrane-spanning helices 5 and 6. Our preliminary data have indicated that the reaction site for SL-H_2DADS-maleimide is on membrane-spanning helix 5 of this model. Given the relative proximity of the covalent reaction sites for BS^3 and SL-H_2DADS-maleimide in the primary structure of band 3, studies were carried out to investigate potential dipolar interactions between SL-H_2DADS-maleimide reacted at the stilbenedisulfonate site and BSSDA reacted at the extracellular monomer−monomer interface. Data obtained from these double spin-labeling experiments (Figure 8) show that the EPR spectrum of [^{15}N,$^2H_{13}$]-SL-H_2DADS-maleimide is unaffected by cross-linking of >85% of the monomers of band 3 by ^{14}N-BSSDA, which supports the conclusion that the nitroxide moieties of [^{15}N,$^2H_{13}$]-SL-H_2DADS-maleimide and ^{14}N-BSSDA are all separated by more than 20 Å. It should be noted that, in all but the most unfavorable geometries (the interelectron vector being at 54.7° with respect to the nitroxide *z*-axes), dipolar interactions should be observable for interelectron distances of 25−30 Å. The spectroscopic arguments leading to this minimum distance of separation have been discussed extensively in previous work (Wojcicki & Beth, 1993a).

It could be argued that a number of different intermolecular cross-link sites exist at the monomer−monomer interface which could be spanned by BSSDA. Such heterogeneity would likely obscure the spectral effects of dipole−dipole interactions due to a superposition of different line shapes. However, even if the distances and angles between the nitroxide moieties of ^{14}N-BSSDA and [^{15}N,$^2H_{13}$]-SL-H_2-DADS-maleimide were different for the different intermolecular cross-linked products, a measurable reduction in the amplitude and/or the broadening of the sharp lines from the EPR spectrum of [^{15}N,$^2H_{13}$]-SL-H_2DADS-maleimide at the stilbenedisulfonate site should be observed if a significant fraction of the BSSDA nitroxides were within 20 Å. The same argument applies if the nitroxide moiety of BSSDA

can exist in different conformations relative to band 3 due to the large number of methylene bonds between the termini of the cross-linking reagent [see Anjaneyulu et al. (1989) for the chemical structure of BSSDA] and also the potential flexibility of the amino acid side chain such as lysine. Since no significant reduction in the amplitude or width of the unique [^{15}N]nitroxide signal was observed following cross-linking of the band 3 monomers by BSSDA, it is unlikely that such cross-linking heterogeneity has affected the interpretation of these double-labeling experiments.

While it is not yet possible to locate the reaction site for SL-H_2DADS-maleimide within the low-resolution structure of the band 3 dimer (Wang et al., 1993, 1994), it is nonetheless interesting to speculate where these sites could be located given the various constraints discussed in the preceding paragraphs. Specifically, the data on inaccessibility of the nitroxide moiety to paramagnetic broadening and chemical-reducing agents in this work, combined with previous energy transfer studies by Rao et al. (1979) and the anti-H_2-DIDS antibody binding studies of Landolt-Marticorena et al. (1995), all indicate that the stilbenedisulfonate site extends into the transmembrane core of band 3. With the constraint that the C_2 symmetry axis bisects both the central "canyon" and the putative extracellular projection of the band 3 dimer in the low-resolution structure of Wang et al. (1994), a concentric region bounded by 20 and 52 Å, the distance constraints determined for the stilbenedisulfonate sites (Macara & Cantley, 1981; Wojcicki & Beth, 1993) include at least a portion of the two prominent extracellular indentations seen in the perspective view of the dimer (Wang et al., 1994). It may be reasonably postulated then that the stilbenedisulfonate sites are in an annular region which is defined by the proximal half of these two extracellular indentations. If it is assumed that the site of BSSDA cross-linking lies near the C_2 symmetry axis, then the distance from the nitroxide moiety of BSSDA at the extracellular protein surface to the nitroxide moieties of SL-H_2DADS-maleimide buried within the transmembrane core of band 3 would also be more than 20 Å if the stilbenedisulfonate sites were located in this 20−52 Å annular region (i.e. all of the distance constraints would be satisfied by this working model). Clearly, more distance constraints are needed to uniquely define the disposition of the sites. However, these data provide important clues for the regions of the known structure to concentrate on in this search.

These studies have described a number of properties of SL-H_2DADS-maleimide which make it a valuable probe of band 3 structure as discussed in the preceding paragraphs. The studies carried out with this new probe have permitted some important conclusions to be drawn about the nature and exposure of the stilbenedisulfonate site and have placed some new restrictions on the spatial disposition of these sites within the overall structure of the band 3 dimer. It is now desirable to expand these studies to include mapping the spatial arrangement of additional sites on band 3 relative to the stilbenedisulfonate sites. One very promising approach for obtaining additional structural information is the use of the site-directed spin-labeling method developed by Hubbell and co-workers [reviewed in Hubbell and Altenbach (1994)]. Recent site-directed mutagenesis studies have been reported (Timmer et al., 1995) where the five endogenous cysteine residues of human band 3 have been replaced with amino acids such as alanine, which would not be expected to react with common spin-labeled sulfhydryl reagents, including spin-labeled maleimides, spin-labeled iodoacetamides, or spin-labeled methanethiosulfonates. These cysteine-less mutant forms have been shown to exhibit normal levels of anion exchange activity (Timmer et al., 1995). If an appropriate expression system can be identified to produce selected single cysteine mutants of band 3, then the full range of studies of accessibility of this unique spin-labeled cysteine to various paramagnetic broadening agents can, in theory, be employed to map the structural and topological characteristics of band 3 in the immediate vicinity. Through production of a number of mutants with unique cysteine residues engineered at selected sites, a wealth of structural information can potentially be obtained as demonstrated in previous studies on bacteriorhodopsin (Altenbach et al., 1989a,b, 1994; Steinhoff et al., 1994) and the ferric enterobactin receptor (Liu et al., 1994). As shown in this work, the accessibility of spin-labeled sites to specifically compartmentalized chemical-reducing agents can add additional insights into the exposure of a site.

The development of SL-H_2DADS-maleimide, combined with its unique labeling properties, suggests a number of double-labeling experiments once site-directed single cysteine mutants are available. Specifically, with [^{15}N,$^2H_{13}$]-SL-H_2-DADS-maleimide reacted at the stilbenedisulfonate site, the distances to other sites, spin-labeled with [^{14}N]nitroxides, within the 10−30 Å range can be investigated through the quantitation of dipole−dipole and exchange interactions using a variety of continuous wave and time domain EPR techniques [general topic reviewed in Eaton and Eaton (1989)].

Beth and Robinson (1989) have provided an extensive discussion of the importance of site-specific labeling of membrane proteins for rigorous interpretation of their anisotropic rotational motion through analysis of ST-EPR data. The work presented here and by Hustedt and Beth (1995, 1996) demonstrates that SL-H_2DADS-maleimide fulfills these labeling specificity requirements. Thus, as shown by previous studies on band 3 rotational dynamics (Hustedt & Beth, 1995), SL-H_2DADS-maleimide will also be a valuable molecular probe for detailed characterization of the global rotational motion of band 3 and hence for addressing questions related to the oligomeric species present in the intact erythrocytes, the mechanical properties of various protein−protein interactions, and the unusual viscoelastic properties of the erythrocyte membrane.

ACKNOWLEDGMENT

The authors thank Dr. Gareth Eaton for providing the Cr(Malt)$_3$ used in these studies, Dr. Mark Jones for his assistance in the synthesis of CuKTSM$_2$, Dr. Jim Feix for providing the TPX capillaries used in these studies, and Scott Blackman for critically reading the manuscript.

REFERENCES

Altenbach, C., Flitsch, S. L., Khorana, H. G., & Hubbell, W. L. (1989a) *Biochemistry 28*, 7806−7812.

Altenbach, C., Marti, T., Khorana, H. G., & Hubbell, W. L. (1989b) *Science 248*, 1088−1092.

Altenbach, C., Greenhalgh, D. A., Khorana, H. G., & Hubbell, W. L. (1994) *Proc. Natl. Acad. Sci. U.S.A. 91*, 1667−1671.

Anjaneyulu, P. S. R., Beth A. H., Cobb, C. E., Juliao, S. F., Sweetman, B. J., & Staros, J. V. (1989) *Biochemistry 28*, 6583−6590.

Appell, K. C., & Low, P. S. (1981) *J. Biol. Chem. 256*, 11104−11111.
Beth, A. H., & Robinson, B. H. (1989) in *Biological Magnetic Resonance: Spin Labeling Theory and Applications, Volume 8* (Berliner, L. J., & Reuben, J., Eds.) pp 179−253, Plenum Press, New York.
Beth, A. H., Balasubramanian, K., Robinson, B. H., Dalton, L. R., Venkataramu, S. D., & Park, J. H. (1983) *J. Phys. Chem. 87*, 359−367.
Beth, A. H., Conturo, T. E., Venkataramu, S. D., & Staros, J. V. (1986) *Biochemistry 25*, 3824−3832.
Burchfield, J., Telehowski, P., Rosenberg, R. C., Eaton, S. S., & Eaton, G. R. (1994) *J. Magn. Reson. B104*, 69−72.
Casey, J. R., & Reithmeier, R. A. F. (1991) *J. Biol. Chem. 266*, 15726−15737.
Casey, J. R., & Reithmeier, R. A. F. (1993) *Biochemistry 32*, 1172−1179.
Casey, J. R., & Kopito, R. R. (1995) *Biophys. J. 68*, A439.
Cherry, R. J., Bürkli, A., Busslinger, M., Schneider, G., & Parish, G. R. (1976) *Nature 263*, 389−393.
Cobb, C. E., & Beth, A. H. (1990) *Biochemistry 29*, 8283−8290.
Cobb, C. E., Hustedt, E. J., Wojcicki, W. E., & Beth, A. H. (1994) *Biophys. J. 66*, A33.
Dix, J. A., Verkman, A. S., Solomon, A. K., & Cantley, L. C. (1979) *Nature 282*, 520−522.
Eaton, G. R., & Eaton, S. S. (1989) in *Biological Magnetic Resonance: Spin Labeling Theory and Applications, Volume 8* (Berliner, L. J., & Reubin, J., Eds.) pp 339−397, Plenum Press, New York.
Fairbanks, G., Steck, T. L., & Wallach, D. F. H. (1971) *Biochemistry 10*, 2606−2617.
Falke, J. J., & Chan, S. I. (1986a) *Biochemistry 25*, 7888−7894.
Falke, J. J., & Chan, S. I. (1986b) *Biochemistry 25*, 7895−7898.
Garcia, A. M., & Lodish, H. F. (1989) *J. Biol. Chem. 264*, 19607−19613.
Gough, T. E. (1973) in *Physical Chemistry of Organic Solvent Systems* (Covington, A. K., & Dickenson, T., Eds.) pp 461−482, Plenum Press, New York.
Griffith, O. H., Dehlinger, P. J., & Van, S. P. (1974) *J. Membr. Biol. 15*, 159−192.
Groves, J. D., & Tanner, M. J. (1994) *J. Membr. Biol. 140*, 81−88.
Haas, D. A., Mailer, C., & Robinson, B. H. (1993) *Biophys. J. 64*, 594−604.
Hubbell, W. L., & Altenbach, C. (1994) in *Membrane Protein Structure: Experimental Approaches* (White, S. H., Ed.) pp 224−248, Oxford University Press, New York.
Hustedt, E. J., & Beth, A. H. (1995) *Biophys. J. 69*, 1409−1423.
Hustedt, E. J., & Beth, A. H. (1996) *Biochemistry 35*, 6944−6954.
Hustedt, E. J., Cobb, C. E., Beth, A. H., & Beechem, J. M. (1993) *Biophys. J. 64*, 614−621.
Jay, D., & Cantley, L. (1986) *Annu. Rev. Biochem. 55*, 511−538.
Jennings, M. L. (1984) *J. Membr. Biol. 80*, 105−117.
Jennings, M. L. (1989) *Annu. Rev. Biophys. Biophys. Chem. 18*, 397−430.
Jennings, M. L., & Nicknish, J. S. (1985) *J. Biol. Chem. 260*, 5472−5479.
Kaufmann, E., Eberl, G., & Schnell, K. F. (1986) *J. Membr. Biol. 91*, 129−146.
Knauf, P. A. (1979) *Curr. Top. Membr. Transp. 12*, 249−363.
Knauf, P. A., Strong, N. M., Penikas, J., Wheeler, R. B., Jr., & Liu, S. J. (1993) *Am. J. Physiol. 264*, C1144−C1154.
Laemmli, U. K. (1970) *Nature 227*, 680−685.
Landolt-Marticorena, C., Casey, J. R., & Reithmeier, R. A. F. (1995) *Mol. Membr. Biol. 12*, 173−182.
Lieberman, D. M., & Reithmeier, R. A. F. (1988) *J. Biol. Chem. 263*, 10022−10028.
Liu, S. J., & Knauf, P. A. (1993) *Am. J. Physiol. 264*, C1155−C1164.
Low, P. S. (1986) *Biochim. Biophys. Acta 864*, 145−167.
Lukacovic, M. F., Feinstein, M. B., Saafi, R. I., & Perrie, S. (1981) *Biochemistry 20*, 3145−3151.
Lux, S. E., John, K. M., Kopito, R. R., & Lodish, H. F. (1989) *Proc. Natl Acad. Sci. U.S.A. 86*, 9089−9093.
Macara, I. G., & Cantley, L. C. (1981) *Biochemistry 20*, 5095−5105.
Macara, I. G., Kuo, S., & Cantley, L. C. (1983) *J. Biol. Chem. 258*, 1785−1792.
Melhorn, R. J. (1991) *J. Biol. Chem. 266*, 2724−2731.
Oikawa, K., Lieberman, D. M., & Reithmeier, R. A. F. (1985) *Biochemistry 24*, 2843−2848.
Okubo, K., Kang, D., Hamasaki, N., & Jennings, M. L. (1994) *J. Biol. Chem. 269*, 1918−1926.
Passow, H. (1986) *Rev. Physiol. Biochem. Pharmacol. 103*, 61−203.
Petering, H. G., Buskirk, H. H., & Underwood, G. E. (1964) *Cancer Res. 24*, 367−372.
Popp, C. A., & Hyde, J. S. (1981) *J. Magn. Reson. 43*, 249−258.
Rao, A., Martin, P., Reithmeier, R. A. F., & Cantley, L. C. (1979) *Biochemistry 18*, 4505−4516.
Reddoch, A. H., & Konishi, S. (1979) *J. Chem. Phys. 70*, 2121−2130.
Schnell, K. F., Käsbauer, W. E., & Kaufmann, E. (1983) *Biochim. Biophys. Acta 732*, 266−275.
Scothorn, D. J., & Beth, A. H. (1994) *Biophys. J. 66*, A33.
Scothorn, D. J., Hustedt, E. J., Cobb, C. E., & Beth, A. H. (1995) *Biophys. J. 68*, A305.
Sekler, I., Lo, R. S., & Kopito, R. R. (1995) *Biophys. J. 68*, A437.
Staros, J. V., & Kakkad, B. P. (1983) *J. Membr. Biol. 74*, 247−254.
Steinhoff, H. J., Mollaaghababa, R., Altenbach, C., Hideg, K., Krebs, M., Khorana, H. G., & Hubbell, W. L. (1994) *Science 266*, 105−107.
Subczynski, W. K., Antholine, W. E., Hyde, J. S., & Petering, D. H. (1987) *J. Am. Chem. Soc. 109*, 46−52.
Subczynski, W. K., Antholine, W. E., Hyde, J. S., & Kusumi, A. (1990) *Biochemistry 29*, 7836−7945.
Tanner, M. J. A., Martin, P. G., & High, S. (1988) *Biochem. J. 256*, 703−712.
Timmer, R. T., Smith, P. A., & Gunn, R. B. (1995) *Biophys. J. 68*, A445.
Van Giessen, G. J., & Petering, H. G. (1968) *J. Med. Chem. 11*, 695−699.
Wang, D. N., Kühlbrandt, W., Sarabia, V. E., & Reithmeier, R. A. F. (1993) *EMBO J. 12*, 2233−2239.
Wang, D. N., Sarabia, V. E., Reithmeier, R. A. F., & Kühlbrandt, W. (1994) *EMBO J. 13*, 3230−3235.
Weinstein, R. S., Khododad, J. K., & Steck, T. L. (1978) *J. Supramol. Struct. 8*, 325−335.
Wojcicki, W. E. (1993) Doctoral Dissertation, Vanderbilt University, Nashville, TN.
Wojcicki, W. E., & Beth, A. H. (1993a) *Biophys. J. 64*, A308.
Wojcicki, W. E., & Beth, A. H. (1993b) *Biochemistry 32*, 9454−9464.

BI960150F